



Cite this: DOI: 10.1039/c5cc09005a

Received 30th October 2015,  
Accepted 20th November 2015

DOI: 10.1039/c5cc09005a

www.rsc.org/chemcomm

Intramolecular electron transfer reactions in  
*meso*-(4-nitrophenyl)-substituted subporphyrins†Graeme Copley,<sup>a</sup> Juwon Oh,<sup>b</sup> Kota Yoshida,<sup>a</sup> Daiki Shimizu,<sup>a</sup> Dongho Kim\*<sup>b</sup> and  
Atsuhiko Osuka\*<sup>a</sup>

**A<sub>2</sub>B-type *meso*-(4-nitrophenyl)-substituted subporphyrins have been synthesized and shown to undergo very fast photoinduced intramolecular charge separation (CS) and charge recombination (CR) between the subporphyrin core and the *meso*-4-nitrophenyl group in CH<sub>2</sub>Cl<sub>2</sub> as probed by femtosecond time-resolved transient absorption spectroscopy. Red-shifted emissions were detected from charge-separated states as a rare case for porphyrinoids.**

Since our initial report describing the synthesis of tribenzosubporphyrins in 2006,<sup>1</sup> much attention has been focused on the exploration of subporphyrins because of their attractive optical, electronic, and structural attributes.<sup>2</sup> A characteristic feature of subporphyrin that is not shared with its older cousin porphyrin is the facile rotation of *meso*-aryl substituents that allows them to exert large electronic influences on the subporphyrin core, drastically altering the properties of the subporphyrin.<sup>3</sup> Prime examples include *meso*-(4-aminophenyl)-substituted subporphyrins and *meso*-(4-oligo(phenylethynyl))-substituted subporphyrins, both of which exhibited perturbed optical and electrochemical properties.<sup>4</sup> Facile rotation of *meso*-aryl groups leads to twisted intramolecular charge transfer in subporphyrins bearing *meso*-arylamino groups.<sup>5</sup> Apart from these accounts, studies on electron transfer reactions of subporphyrins have been rather limited, while significant fluorescence quenching of subporphyrins has been observed in several cases.<sup>6,7</sup>

In this work, we have focused on a set of A<sub>2</sub>B-type subporphyrins bearing *meso*-4-nitrophenyl groups (Fig. 1) paying particular attention to intramolecular electron transfer reactions. While *meso*-4-nitrophenyl-substituted subporphyrin was previously prepared and its significant fluorescence quenching in CH<sub>2</sub>Cl<sub>2</sub> was noted,<sup>7</sup> the photo-excited-state dynamics were

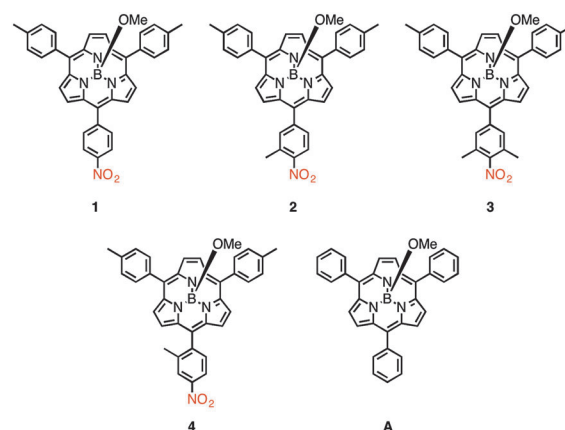


Fig. 1 The molecular structures of the subporphyrins described in this study.

not examined in detail. In subporphyrins 1–3, the 4-nitrophenyl groups are free to rotate at will, maximising their electronic influence on the subporphyrin core. However, the rotational freedom of the nitro groups in 2 and 3 is different, since the introduced methyl groups in 2 and 3 decrease the rotational freedom. In 4, the 2-methyl group imposes a severe rotational barrier of the *meso*-aryl substituent, enforcing an orthogonal conformation.<sup>8</sup>

Subporphyrins 1–4 were synthesized by following improved protocols for realizing A<sub>2</sub>B type subporphyrins in 16, 8, 7, and 3% yields, respectively. The purity and authenticity of 1–4 have been unambiguously confirmed by <sup>1</sup>H, <sup>11</sup>B, <sup>13</sup>C NMR spectroscopy, and high-resolution atmospheric-pressure-chemical-ionization (HR-APCI-TOF) mass spectrometry (Fig. S2 and S3 in the ESI†). The <sup>1</sup>H NMR spectrum of 4 displays signals corresponding to both *exo*- and *endo*-atropisomers in a 4:1 ratio in CDCl<sub>3</sub> at room temperature (Fig. S2–S10 in the ESI†). The <sup>1</sup>H NMR spectrum of compound 4 remained unchanged upon elevating to high temperatures, indicating a high rotational barrier of the 2-methyl-4-nitrophenyl substituent. Single crystals of 1 suitable for X-ray diffraction analysis were obtained by slow diffusion of

<sup>a</sup> Department of Chemistry, Graduate School of Science, Kyoto University, Kyoto 606-8502, Japan. E-mail: souk@kuchem.kyoto-u.ac.jp

<sup>b</sup> Department of Chemistry, Yonsei University, Seoul 120-749, Korea. E-mail: dingo@yonsei.ac.kr

† Electronic supplementary information (ESI) available. CCDC 1429320. For ESI and crystallographic data in CIF or other electronic format see DOI: 10.1039/c5cc09005a

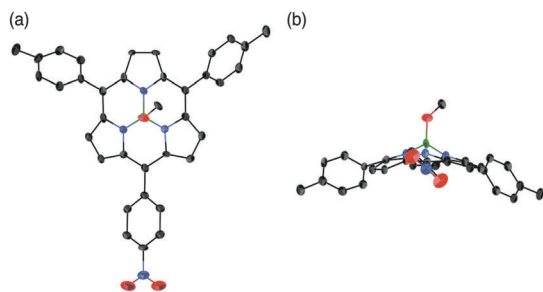


Fig. 2 X-Ray crystal structure of **1** (a: top view, b: side view). The molecular structure shown is one of the two independent molecules in the unit cell. Thermal ellipsoids are set at 50% probability level. Hydrogen atoms and solvent molecules are omitted for clarity.

pentane into a solution of **1** in benzene (Fig. 2). The average bowl depth was calculated to be  $1.34 \text{ \AA}^9$  whilst the dihedral angle of the 4-nitrophenyl group was determined to be  $41.97^\circ$ . These values are consistent with the ground state optimized geometry (see below).

Using the crystal structure of **1** as a starting point, optimised ground state structures of **1–4** have been calculated using the Gaussian 09 program package (Fig. S8-1 in ESI†). The dihedral angles of the *meso*-4-nitrophenyl groups in **1–3** were calculated to be  $44.6^\circ$ ,  $44.3^\circ$ , and  $45.2^\circ$ , respectively, suggesting that the *meso*-4-nitrophenyl groups in **1–3** possess very similar rotational freedom.

The dihedral angles between the nitro group and its respective aryl group in **1–3** were calculated to be  $0.5^\circ$ ,  $12.3^\circ$ , and  $42.9^\circ$ , respectively. This ascending trend is in line with the systematic introduction of methyl groups adjacent to the nitro group, gradually increasing steric hindrance. As anticipated, the dihedral angle between the 2-methyl-4-nitrophenyl group and the subporphyrin core was calculated to be  $58.2^\circ$ , much larger than the dihedral angles observed for **1–3** ( $44.6^\circ$ ,  $44.2^\circ$ , and  $45.2^\circ$ ). This can be ascribed to the steric clash between the 2-methyl group and the subporphyrin periphery. The dihedral angle of the nitro group and its respective aryl group in **4** was calculated to be just  $0.7^\circ$ , indicating that a coplanar relationship is favoured as in the case of **1**. Despite their individual structural features, the molecular orbital diagrams calculated for **1–4** suggest that all of the compounds share a similar intramolecular charge transfer character (Fig. S8-2 in the ESI†). In the HOMO plots for **1–4**, electron density is distributed over the entirety of the molecular framework. In the LUMO plots for **1–4**, electron density appears to be pulled on to the electron withdrawing *meso*-4-nitrophenyl substituents and away from the subporphyrin cores.

Fig. 3 shows the absorption and emission spectra of **1–4** along with a reference compound triphenylsubporphyrin **A** in  $\text{CH}_2\text{Cl}_2$  (an important observation to note is that the absorption spectra of **1–4** recorded in  $\text{CH}_2\text{Cl}_2$  were practically the same as those recorded in toluene (Fig. S7-1 in the ESI†)). The Soret-like band of **1** is the broadest in the set, indicating the largest electronic interaction between the 4-nitrophenyl group and the subporphyrin core. There is a visible sharpening of the

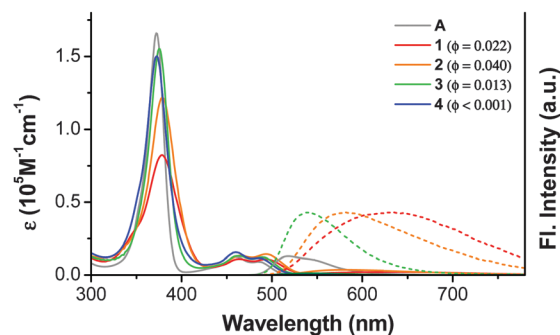


Fig. 3 Absorption (solid) and emission (dashed) spectra of compounds **1–4**, along with control compound **A**, recorded in  $\text{CH}_2\text{Cl}_2$ .

Soret-like band and overall absorption spectra moving through **1–3**, and a slight broadening again for **4**. The full width at half maximum (FWHM) values for **1**, **2**, **3** and **4** are  $2870$ ,  $2309$ ,  $1785$ , and  $1993 \text{ cm}^{-1}$ , respectively. This sharpening trend in **1–3** can be ascribed to the dwindling electronic influence of the nitro group on the subporphyrin core due to the increasing steric constraint. The  $\lambda_{\text{max}}$  value of  $372 \text{ nm}$  and the molar extinction coefficient value of  $1.50 \times 10^5 \text{ M}^{-1} \text{ cm}^{-1}$  for **4** highlights the decoupled nature of the *meso*-2-methyl-4-nitrophenyl group and the subporphyrin core. In comparison to **3**, a slight broadening of the absorption profile for **4** is most likely due to the presence of its atropisomers (Table 1).

In non-polar toluene, the emission maxima for **1–4** were observed at  $542$ ,  $546$ ,  $533$ , and  $533 \text{ nm}$  with the fluorescence quantum yields recorded as  $0.28$ ,  $0.26$ ,  $0.22$ , and  $0.23$ , respectively. Compared to **A**, increased fluorescence quantum yields of **1–4** suggest that a perturbation effect is introduced by the presence of the 4-nitrophenyl groups, where the higher quantum yields of **1** and **2** in comparison to **3** and **4** can be ascribed to the restricted influence of the nitro groups on the subporphyrin core in **3** and **4**. In contrast, the fluorescence emissions of **1–4** are all significantly quenched in moderately polar  $\text{CH}_2\text{Cl}_2$  ( $0.022$ ,  $0.040$ ,  $0.013$ , and  $<0.001$  for **1–4**, respectively) with their fluorescence emission spectra becoming significantly broadened and red-shifted. Such spectral features suggest the occurrence of efficient intramolecular charge transfer processes in **1–4**. Again, a nice trend can be observed for the broadening and red-shifting of the emission profiles with respect to **1–3**, with **1** exhibiting the most broadened and most red-shifted emission profile.

The electrochemical properties of **1–4** along with the reference subporphyrin **A** were investigated by cyclic voltammetry (CV) measurements in  $\text{CH}_2\text{Cl}_2$  and the results are listed in Table 2.

Table 1 Photophysical parameters of compounds **1–4**. Values were recorded in  $\text{CH}_2\text{Cl}_2$  unless stated

Comp.	$\lambda_{\text{max}}/\text{nm}$	FWHM/ $\text{cm}^{-1}$	$\epsilon/\text{M}^{-1} \text{ cm}^{-1}$	$\Phi_{\text{F}}$ in $\text{CH}_2\text{Cl}_2$	$\Phi_{\text{F}}$ in toluene
<b>1</b>	378, 464, 493	2870	$8.20 \times 10^4$	0.022	0.28
<b>2</b>	379, 464, 493	2309	$1.22 \times 10^5$	0.040	0.26
<b>3</b>	375, 463, 489	1785	$1.55 \times 10^5$	0.013	0.22
<b>4</b>	372, 460, 485	1993	$1.50 \times 10^5$	$<0.001$	0.23
<b>A</b>	373, 461, 484	1527	$1.66 \times 10^5$	0.14	0.16

**Table 2** Redox potentials of **1–4** in CH<sub>2</sub>Cl<sub>2</sub> measured by cyclic voltammetry<sup>a</sup> and estimated energy levels of CSS and  $-\Delta G^\circ$  for charge separation

Compound	$E^{1/2}_{\text{OX1/V}}$	$E^{1/2}_{\text{RED1/V}}$	$E^{1/2}_{\text{RED2/V}}$	CSS/eV	$-\Delta G^\circ$ (eV)
<b>1</b>	0.78	$-1.36^b$	$-1.56^b$	1.86	−0.49
<b>2</b>	0.72	−1.74		2.18	−0.19
<b>3</b>	0.70	−1.79		2.21	−0.21
<b>4</b>	0.71	−1.69	−1.96	2.12	−0.25
<b>A</b>	0.71	−1.97			

<sup>a</sup> Conditions: scan rate: 0.05 V s<sup>−1</sup>, supporting electrolyte: 0.1 M *n*Bu<sub>4</sub>NPF<sub>6</sub>, working/counter electrodes: Pt/Pt wire, reference electrode: Ag/0.01 M AgClO<sub>4</sub> in MeCN. <sup>b</sup> Determined by differential pulse voltammetry.

The first oxidation waves of **1**, **2**, and **3** were observed at 0.78, 0.72, and 0.70 V, respectively, reflecting the decreasing influence of the nitro group due to the installed methyl groups, in this order. In the reduction part, **1** showed two reversible reduction waves at  $-1.36$  V and  $-1.56$  V. By searching the existing literature, these two reduction waves have been assigned to the reduction of the freely rotating 4-nitrophenyl group and of the electron deficient subporphyrin core, respectively.<sup>10</sup> In **2**, the installed methyl group mitigates communication between the nitro group and aryl group. Judging from the first oxidation and reduction potentials of 0.72 and  $-1.74$  V, the nitro group in **2** is exerting a modest influence on the subporphyrin core. The influence of the nitro group in **3** is even less due to the two methyl groups flanking the nitro group. Finally, the oxidation potential of **4** was observed at 0.71 V, whilst the reduction potentials were observed at  $-1.69$  and  $-1.96$  V. These values confirm that the 2-methyl-4-nitrophenyl group in **4** is electronically decoupled from the subporphyrin core, although the nitro group can still influence its respective aryl group due to the absence of methyl groups at the 3 and 5 positions. On the basis of the above electrochemical data, the energy levels of the charge separated states (CSS), consisting of a subporphyrin cation radical and a nitrobenzene anion radical, have been estimated to be 1.86, 2.18, 2.21, and 2.12 eV for **1–4**, respectively (Coulombic correction term was taken into account when calculating these values (Table 2)). These considerations made it possible to estimate the driving force for CS to be  $-0.49$ ,  $-0.19$ ,  $-0.21$ , and  $-0.25$  eV for **1–4**, respectively.

To reveal the CS and CR events in **1–4**, femtosecond transient absorption (TA) spectra were recorded in CH<sub>2</sub>Cl<sub>2</sub> (Fig. 4 and Fig. S7-2 in the ESI<sup>†</sup>). As a control experiment, a

subporphyrin cation radical generated by chemical oxidation of **A** with NOSbF<sub>6</sub> displayed absorption bands at 388 and 502 nm (Fig. S6-1 in the ESI<sup>†</sup>). After searching the literature, the electrochemically generated radical anion of nitrobenzene showed absorption bands at 435 and 465 nm with a tail reaching out to 600 nm.<sup>11</sup> The TA spectra of **1** displayed very rapid formation and decay of the CS state showing broad absorbance in the range of 500–630 nm consisting of contributions from the subporphyrin cation radical and the nitrobenzene anion radical with a CS rate of  $(3.7 \text{ ps})^{-1}$  and a CR rate of  $(330 \text{ ps})^{-1}$ . The TA spectra of **2** and **3** also revealed quantitative CS and CR with  $k_{\text{CS}} = (3.0 \text{ ps})^{-1}$  and  $k_{\text{CR}} = (530 \text{ ps})^{-1}$  for **2**, and  $k_{\text{CS}} = (2 \text{ ps})^{-1}$  and  $k_{\text{CR}} = (210 \text{ ps})^{-1}$  for **3**, respectively. The fluorescence lifetimes of **1–3** (340, 510, and 200 ps, respectively) were all well matched with the lifetimes for CR processes, indicating that their red-shifted fluorescence in CH<sub>2</sub>Cl<sub>2</sub> is originating from the CS state (Fig. S7-3 in the ESI<sup>†</sup>). It is worth noting that such CR-associated emissions<sup>12</sup> have been very rare for porphyrins. The TA spectra of **4**, which is held in an orthogonal conformation, also indicated the rise and decay of broad absorbance in the range of 480 nm to 660 nm due to the CS state with  $k_{\text{CS}} = (5.0 \text{ ps})^{-1}$  and  $k_{\text{CR}} = (40 \text{ ps})^{-1}$ . Very fast CR in **4** may explain its non-fluorescence nature in the red-shifted region due to its short lived CS state. Therefore, it may be inferred that weak CR-associated emission is only allowed for subporphyrins bearing freely rotating *meso*-aryl groups.

In summary, A<sub>2</sub>B-type *meso*-(4-nitrophenyl)-substituted subporphyrins **1–4** have been synthesized and have been shown to undergo very fast photoinduced intramolecular CS and CR reactions between the subporphyrin core and the *meso*-4-nitrophenyl group in CH<sub>2</sub>Cl<sub>2</sub>. Characteristically, broad and red-shifted emissions were detected from the CS states of **1–3** as a rare case for porphyrinoids.

The work at Kyoto was supported by JSPS KAKENHI Grant Numbers (25220802 and 25620031). The work at Yonsei was supported by Global Research Laboratory (GRL) Program (2013K1A1A2A02050183) through the National Research Foundation of Korea (NRF) funded by the Ministry of Science, ICT (Information and Communication Technologies) and Future Planning. GC thanks JSPS for a Postdoctoral Fellowship.

## Notes and references

- Y. Inokuma, J. H. Kwon, T. K. Ahn, M.-C. Yoo, D. Kim and A. Osuka, *Angew. Chem., Int. Ed.*, 2006, **45**, 961.
- (a) T. Torres, *Angew. Chem., Int. Ed.*, 2006, **45**, 2834; (b) Y. Inokuma and A. Osuka, *Dalton Trans.*, 2008, 2517; (c) A. Osuka, E. Tsurumaki and T. Tanaka, *Bull. Chem. Soc. Jpn.*, 2011, **84**, 679; (d) C. G. Claessens, D. González-Rodríguez, M. S. Rodríguez-Morgade, A. Medina and T. Torres, *Chem. Rev.*, 2014, **114**, 2192; (e) N. Kobayashi, Y. Takeuchi and A. Matsuda, *Angew. Chem., Int. Ed.*, 2007, **46**, 758.
- Y. Inokuma, Z. S. Yoon, D. Kim and A. Osuka, *J. Am. Chem. Soc.*, 2007, **129**, 4747.
- (a) Y. Inokuma, S. Easwaramoorthi, S. Y. Jang, K. S. Kim, D. Kim and A. Osuka, *Angew. Chem., Int. Ed.*, 2008, **47**, 4840; (b) Y. Inokuma, S. Easwaramoorthi, Z. S. Yoon, D. Kim and A. Osuka, *J. Am. Chem. Soc.*, 2008, **130**, 12234.
- (a) M. Kitano, S. Hayashi, T. Tanaka, N. Aratani and A. Osuka, *Chem. – Eur. J.*, 2012, **18**, 8929; (b) W.-Y. Cha, J. M. Lim, K. H. Park, M. Kitano, A. Osuka and D. Kim, *Chem. Commun.*, 2014, **50**, 8491.

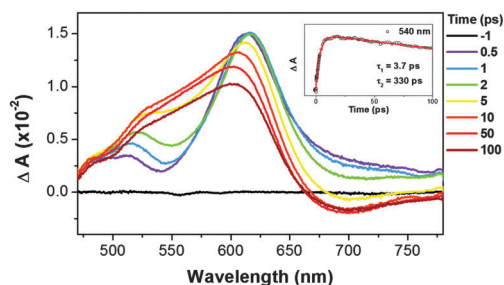


**Fig. 4** TA spectra and decay profile (inset) of **1** in CH<sub>2</sub>Cl<sub>2</sub> (excitation at 490 nm).

- 6 (a) H. Sugimoto, T. Tanaka and A. Osuka, *Chem. Lett.*, 2011, **40**, 629; (b) S. Saga, S. Hayashi, K. Yoshida, E. Tsurumaki, P. Kim, Y. M. Sung, J. Sung, T. Tanaka, D. Kim and A. Osuka, *Chem. – Eur. J.*, 2013, **19**, 11158; (c) D. Shimizu, H. Mori, M. Kitano, W.-Y. Cha, J. Oh, T. Tanaka, D. Kim and A. Osuka, *Chem. – Eur. J.*, 2014, **20**, 16194.
- 7 T. Tanaka, M. Kitano, S. Hayashi, N. Aratani and A. Osuka, *Org. Lett.*, 2012, **14**, 2694.
- 8 K. Yoshida, G. Copley, H. Mori and A. Osuka, *Chem. – Eur. J.*, 2014, **20**, 10065.
- 9 The bowl depth of the subporphyrin is defined as the vertical distance between the mean plane of the six  $\beta$  carbon atoms and the central boron atom.
- 10 A. Kuhn, K. G. von Eschwege and J. Conradie, *J. Phys. Org. Chem.*, 2012, **25**, 58.
- 11 W. Kemula and R. Sioda, *Nature*, 1963, **197**, 588.
- 12 (a) P. Pasman and J. W. Verhoeven, *J. Am. Chem. Soc.*, 1982, **104**, 5127; (b) P. Pasman, G. F. Mes, N. W. Koper and J. W. Verhoeven, *J. Am. Chem. Soc.*, 1985, **107**, 5839.